TRANSITION EFFECT AT THE MEDIUM—VACUUM INTERFACE UNDER THE SELF-PHASE MODULATION OF A LIGHT PULSE

S.O. DUDKA, A.I. IVANISIK, A.V. KONOPATSKIY, P.A. KOROTKOV

Taras Shevchenko Kyiv National University, Faculty of Radiophysics
(2, Build. 5, Academician Glushkov Ave., Kyiv 03127, Ukraine)

UDC 535.2:621.373.8

The phase self-modulation of nanosecond laser pulses under the quasi-stationary self-focusing in the Kerr liquid has been studied. Computations of the additional phase delay, the instantaneous frequency, and the pulse spectrum have been carried out. The results of computations and the experimental data obtained evidence for the existence of the transition effect which promotes the appearance of new spectral components at the medium boundary. The spectral components, which arise owing to this effect, have the Stokes shift of about 100 cm^{-1} with respect to the exciting radiation frequency. Notwithstanding the possible significant frequency broadening of the pulses, the spectral energy density remains maximal at the unshifted frequency.

1. Introduction

The phase modulation (PM) of laser pulses stemming from self-focusing (SF) has been studied for a long time, which was described in monographs [1, 2]. The importance of the issue is stimulated by practical implications of PM and SF and by the fact that, under typical conditions, SF governs the threshold for other nonlinear optical processes such as stimulated Raman spectroscopy (SRS) [3], stimulated Brillouin scattering [3], etc. and essentially affects their efficiency. Nevertheless, the developed ideas of the PM of nanosecond pulses in Kerr liquids possess a qualitative character and partially consider changes in the arrangement and the dimensions of the focal area, which depend on the instant emission power.

We note that the matter concerns, first of all, PM under conditions of the quasi-stationary SF which is realized for pulses with the duration $\tau \geq 1$ ns, i.e. much longer that the time constant of the Kerr effect in liquids (about $1 - 10$ ps). The theory of PM under the quasi-stationary SF is developed better [2]. The ultrashort pulses are spatially compressed in the course of SF, and the distribution of the pulse field intensity remains constant afterwards (if the dispersive smearing is not taken into account). Such a pulse moves having the horn-like shape, and, after changing over to the "accompanying" coordinate system, the problem becomes stationary (the stationary mode of the nonlinear propagation of the pulse). The PM of ultrashort pulses is considered to be responsible for the generation of a spectral continuum about 1000 cm^{-1} in width [1, 2, 4]. In particular, the PM of pulses with a duration of about 5 ps stimulates the emission possessing the shift $\Delta\nu \approx 100$ cm^{-1} with respect to the initial frequency [5].

In the case of the quasi-stationary SF, where every time fragment of the pulse self-focuses, in a first approximation, irrespectively of the others, and the resulted contribution to the refractive index is determined according to stationary conditions, it is necessary to consider the nonstationarity which is connected with changes of both the spatial distribution of the field in the focal area and its arrangement owing to the variation of the instant power of the pulse. In this case, making use of the "accompanying" coordinate system does not simplify the problem.

The problem also becomes complicated, because the reliable data concerning the field distribution in the focal area and behind it are absent. The theory works satisfactorily in the prefocal region. Taking into account only the effects of diffraction and nonlinear refraction results in the unlimited growth of the field amplitude at the focus. The question what universal physical mechanism defines the minimal radius of the focal area remains unanswered ultimately, which constrains the opportunities to describe the behavior of the beam behind the focal area.

In general, the existing ideas of the quasi-stationary PM as a result of SF are based, on the one hand, on ignoring changes in the arrangement and the dimensions of the focal area in the framework of the pulse self-channeling model and on taking into account only variations in the radiation power in the stationary channel [6], and, on the other hand, on the exaggeration of the role of the focal area motion during the period when the induced contribution to the refractive index achieves its stationary value [1]. In both cases, the

authors adhere to the conclusion about the smooth bell-shaped form, with a single maximum, of the function of the additional phase delay in time and the corresponding spectrum of emission, which contains (without taking into account the orientation inertia of molecules) two the most intense symmetric components with the frequency shift $\Delta\nu \approx \pm 100$ cm^{-1}. The spectral energy of these components exceeds the spectral energy of radiation at the laser frequency. This contradicts the well-known experimental data that, while leaving from the medium, the energy of radiation with $\Delta\nu = 0$ is the highest, similarly to the energy of the SRS Stokes and anti-Stokes components at combination frequencies [7].

In this work, we propose a simplified but more adequate (in our opinion) model of PM under the quasi-stationary SF and discuss the experimental data that evidence for the occurrence of the transition effect which promotes the generation of new spectral components at the medium boundary, provided the phase self-modulation of nanosecond pulses of the laser emission.

2. Theoretical Background

In order to calculate the extra phase incursion $\Delta\varphi(t, L)$, which the pulse possessing the power $P(t)$ that varies in time t acquires at the outlet point of the medium of length L, we use the well-known results. The critical power $P_{\rm cr}$ of SF for a Gaussian-like beam with a flat phase front in a medium, whose refractive index $n = n_0 + n_2 E_0^2$ depends on the strength peak value E_0 of the electric field of a wave, is equal to (in SI units) [1]

$$P_{\rm cr} = \frac{\pi(1.22\lambda_0)^2}{32\mu_0 n_2 c}, \tag{1}$$

where λ_0 is the wavelength, c the velocity of light, n_2 the quantity derived from the Kerr constant, and $\mu_0 = 4\pi \times 10^7$ H/m. Provided that $\tilde{P} = P/P_{\rm cr} \geq 1$, the focal point arises at the distance

$$z_f = 0.367 n_0 k_0 a_0^2 \Big/ \left[(\sqrt{\tilde{P}} - 0.852)^2 - 0.0219\right]^{1/2} \tag{2}$$

from the inlet boundary [8], where $k_0 = 2\pi/\lambda_0$ and a_0 is the initial radius of the beam.

The intensity $I(z)$ along the coordinate z of the beam axis in the prefocal region amounts to [8]

$$I(z)/I(0) = \left[1 - (z/z_f)^2\right]^{-\mu/2}. \tag{3}$$

Applying the results of work [8], the dependence of the parameter μ on the parameter $\tilde{P}$ within the interval $1.3 \leq \tilde{P} \leq 10$ can be approximated by the function

$$\mu = 2.9\tilde{P}^{-0.5} + \tilde{P}^{-1} + 1 \tag{4}$$

with an accuracy of about 1%.

According to experimental data [1], the minimal radius a_f of the focal region is characteristic of every specific medium and does not depend on $\tilde{P}$.

The behavior of the beam behind the focal point has been not studied yet. Let us suppose that the focal region is symmetric, and, therefore, the beam diverges behind the focal point in the same manner as it converges just before it. Such an assumption is justified, because the beam undergoes losses in the focal region owing to the nonlinear scattering processes, and the self-channeling does not occur.

Taking into account the above-stated, the dependence $a_z^2(z)$ is approximated by the function

$$a_z^2 = \left(a_0^2 - a_f^2\right)\left|1 - (z/z_f)^2\right|^{\mu/2} + a_f^2. \tag{5}$$

The confocal parameter (the distance between points, where $a_z = \sqrt{2}a_f$) of beam (5) is equal to

$$\ell \approx \quad z_f (a_f/a_0)^{4/\mu}. \tag{6}$$

Knowing a_z, one can estimate the intensity $I(z)$ at the beam axis ($I(z) \approx P/(\pi a_z^2)$), find the amplitude of the field ($E_0(z)^2 = 2c\mu_0 I(z)/n_0$), and calculate the contribution to the refractive index ($\Delta n(z) = n_2 E_0(z)^2$). In this case, if the inertia of the Kerr effect at the cell outlet owing to PM is not taken into account, the extra phase incursion is

$$\Delta\varphi(L,t) = k_0 \int_0^L \Delta n dz = k_0 \tilde{P}(t) \frac{(1,22\lambda_0)^2}{16 n_0} \int_0^L \frac{1}{a_z^2} dz. \tag{7}$$

PM leads to the frequency modulation. The instant frequency offset (in units of cm^{-1}) is

$$\Delta\nu(t) = -\frac{1}{2\pi c}\frac{\partial(\Delta\varphi)}{\partial t}. \tag{8}$$

At the medium outlet, the distribution of the spectral density of the pulse energy $W(\Delta\nu)$ is determined by the Fourier transformation

$$W(\Delta\nu) \sim \left| \int_{-\infty}^{\infty} \sqrt{\tilde{P}(t)} \exp[i(2\pi c \Delta\nu t + \Delta\varphi(t))] dt \right|^2. \tag{9}$$

In Fig. 1, the plot of the function $\Delta\varphi(L,t)$ is presented for the pulse $P(t) \sim \exp(-t^2/\tau^2)$ and

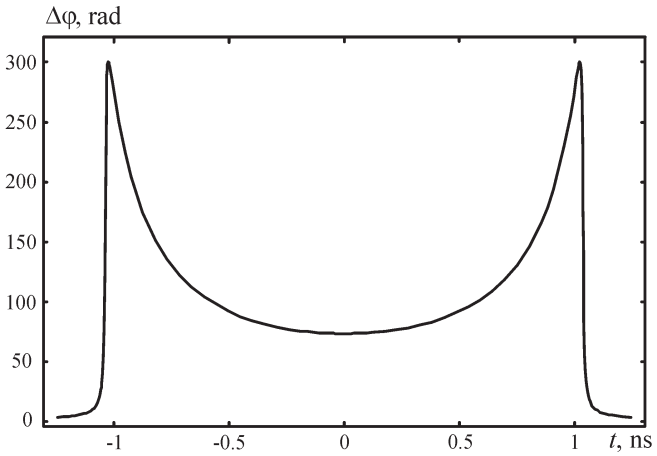

Fig. 1. Dependence of the extra phase incursion $\Delta\varphi$ on the time t for a Gaussian-like pulse; $\tau = 1$ ns, $L = 0.3$ m, $\tilde{P} = 3.6$, $a_0 = 113$ μm, $a_f = 5$ μm, $n_0 = 1.49$, and $\lambda_0 = 0.69$ μm

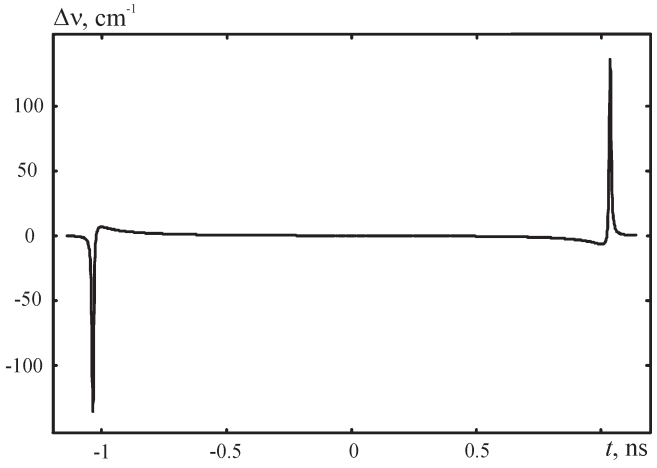

Fig. 2. Variation of the instant frequency offset during the pulse (corresponds to $\Delta\varphi$ in Fig. 1)

provided typical parameters of PM emission of a ruby laser in toluene [9]: $\tau = 1$ ns, $L = 0.3$ m, $\tilde{P} = 3.6$, $a_0 = 113$ μm, $a_f = 5$ μm, $n_0 = 1.49$, and $\lambda_0 = 0.69$ μm. The function $\Delta\varphi(L,t)$ has two maxima: on the front and back sides of the pulse, if the focal region is located near the medium boundary. This is explained by a quick growth of the confocal parameter ℓ (6) of the beam as the power $P(t)$ drops down. Generally, the function $\Delta\varphi(L,t)$ attains its minimal value at the top of the pulse.

The time dependence $\Delta\nu(t)$ for the function $\Delta\varphi(L,t)$ exposed in Fig. 1 is depicted in Fig. 2. The offset of the instant frequency of the laser emission has four maxima. Two the largest, which achieve $\Delta\nu_{\max}(t) \sim \pm 100$ cm^{-1}, are a consequence of the transition effect at the phase self-modulation, the effect being connected with the

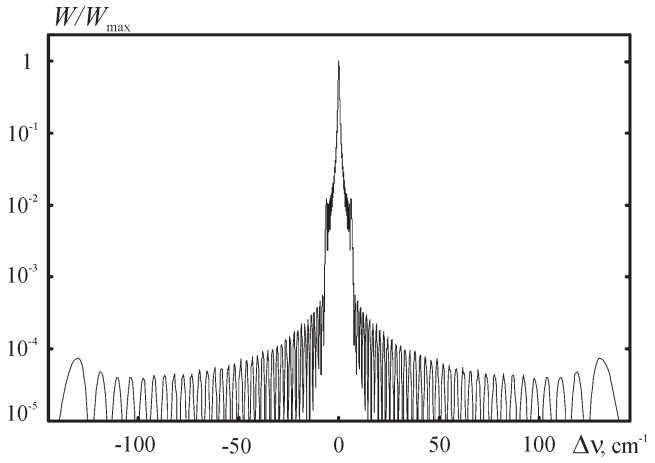

Fig. 3. Normalized distribution of the spectral density of the pulse energy W (corresponds to $\Delta\varphi$ in Fig. 1)

crossing of the medium boundary by the focal region. The substantial frequency offset is a result of the fast variation of the length of that part of the focal region, which is located in the medium. The dependence $\Delta\nu_{\max}(t)$ is negative on the front of the pulse and positive on its back. The other two maxima reach about ± 10 cm^{-1} and appear if the whole focal region is already in the medium. These maxima are caused by a fast reduction of the parameter ℓ as P increases and by the change of the sign of $\Delta\nu(t)$.

While calculating the spectrum (Fig. 3), the integration in Eq. (9) was carried on over the time interval, where $\tilde{P} \geq 1$. Therefore, it is the spectrum of that part of the laser pulse, for which SF plays an appreciable role. One should pay attention that, provided typical experimental conditions, the spectrum includes an unshifted component, about 1 cm^{-1} in width for nanosecond pulses. The spectral energy density W of this component is several orders of magnitude higher than that in the other sections of the spectrum. Within the range of frequencies which are caused by the transition effect, W can achieve about 0.1% of the maximal value $W_{\max}$ only if the specific experimental conditions has been provided, and $0.01 - 0.001\%$ otherwise. Concerning the frequencies in the vicinity of about 10 cm^{-1}, which are generated on the front and the back of the pulse owing to the fast reduction of ℓ, $W/W_{\max} \sim 1\%$ in this section of the spectrum even under typical experimental conditions.

For the maximal value $\Delta\nu_{\max}(t)$ caused by the transition effect, it is possible to derive an analytical expression, starting from the following considerations.

The increment of the refractive index in the focal point is known:

$$\Delta n_f = n_2 E_0(z_f)^2 = \gamma \tilde{P}, \tag{10}$$

where

$$\gamma \equiv (1.22\lambda_0/a_f)^2/16n. \tag{11}$$

At the distance $\delta z = z - z_f$ from the center of the focal region, if it is considered cylindrical with the radius a_f (the smaller is δz, the better this assumption is satisfied), the extra phase incursion $\Delta\varphi(z_f + \delta z)$ is connected with $\Delta\varphi(z_f)$ by the relationship

$$\Delta\varphi(z_f + \delta z) = \Delta\varphi(z_f) + k_0 \Delta n_f \delta z. \tag{12}$$

The calculations carried out making use of Eq. (7) showed that the extra phase incursion $\Delta\varphi(z_f)$ at the focal point is proportional to z_f, namely,

$$\Delta\varphi(z_f,\ t) = k_0 \beta z_f(t), \tag{13}$$

where β is the coefficient which practically does not depend on $\tilde{P}(t)$ and is approximated by the expression

$$\beta = \frac{0,28}{n}\left(\frac{1,22\lambda_0}{a_0}\right)^2\left(\frac{a_0}{a_f}\right)^{2/3}. \tag{14}$$

Substituting Eqs. (10) and (13) into Eq. (12), we obtain the following expression for the extra phase incursion near the center of the focal region:

$$\Delta\varphi(z_f + \delta z) = k_0(\beta z_f + \gamma \delta z \tilde{P}). \tag{15}$$

Thus, at the moment when the central part of the focal region crosses the medium boundary located at $z = L$, the offset of the instant frequency of the axial laser emission at the medium outlet is equal to [8]

$$\Delta\nu_{\max} = -\frac{k_0}{2\pi c}[\beta v_f + \gamma \delta z \frac{d\tilde{P}}{dt} - \gamma v_f \tilde{P}], \tag{16}$$

where $v_f = \frac{dz_f}{d\tilde{P}}\frac{d\tilde{P}}{dt}$ is the velocity of the focal point at the medium boundary (without taking into account the difference between times which are necessary for the pulse fragments to reach the focal point) and $\delta z = L - z_f$.

Not all the terms in Eq. (16) are equally substantial. The third term is significantly greater than the first one, because the increment $\gamma\tilde{P}$ of the refractive index at the focal point considerably exceeds the arithmetic-mean increment β of the refractive index at the interval between the inlet boundary of the medium and the focal point. Concerning the second term, $\delta z = L - z_f \to 0$ in the adjacent neighborhood of the focal point, so that this term can also be neglected in our case. As a result of those simplifications, we obtain (in units of cm^{-1})

$$\Delta\nu_{\max} \approx \frac{k_0}{2\pi c}\gamma \tilde{P} v_f. \tag{17}$$

In relation (17), the values of the parameters $\tilde{P}$ and v_f correspond to the moment, when $z_f = L$. The velocity v_f is positive if the focal point moves in the direction of the laser beam propagation.

3. Experimental Results

To study the transition effect at the phase self-modulation, we used a ruby laser with an $8 \times 120\text{-mm}^2$ active element, a 34-cm linear resonator, and passive Q-switching. The laser emitted pulses with the wavelength $\lambda_0 = 0.6943$ μm, the maximal energy $E_{i,\max} = 0.55$ J, and the duration of 30 ns at the half-peak level. The shape of a laser pulse was smooth, but contained insignificant oscillations with a period of about 2 ns. In its cross-section, the laser beam was non-uniform, with a plenty (about 10^2) of intensity maxima and minima. The width of the laser generation spectrum was 0.01 cm^{-1} at its half-peak level, which did not exceed the spectral distance between two neighbor longitudinal modes. Nevertheless, a weak lateral longitudinal mode was observed at a distance $\delta\nu_{\mathrm{m}} = 0.0156$ cm^{-1} from the central one. Provided such a mode content, the pulse envelope may contain oscillations with the period $T = 1/(\delta\nu_m c) = 2.14$ ns.

The laser emission, when required, was attenuated and directed into a cell with the length $L = 25$ or 12 cm, filled with toluene and located at a distance of about 1 m from the laser. The outlet boundary of the cell was projected without magnification onto the slit of a spectrograph making use of a lens with a focal length of 10 cm. The reciprocal linear dispersion of the spectrograph was 1.33 nm/mm, and the aperture angle $70'$. In the focus of the projecting lens and perpendicularly to the spectrograph slit, there was a screen in the form of a 2.5-mm strip in order to absorb the rather intense axial radiation within the angle range of $\pm 40'$. The spectra were registered by a digital camera from the surface of a scattering glass located in the cassette part of the spectrograph. The spectrograph's slit width was 100 μm, which restricted the spectral resolution to 0.13 nm. Nevertheless, a more essential restriction to 0.2 nm was caused by the application of the scattering glass. The same factor resulted in a spatial resolution of about 150 nm.

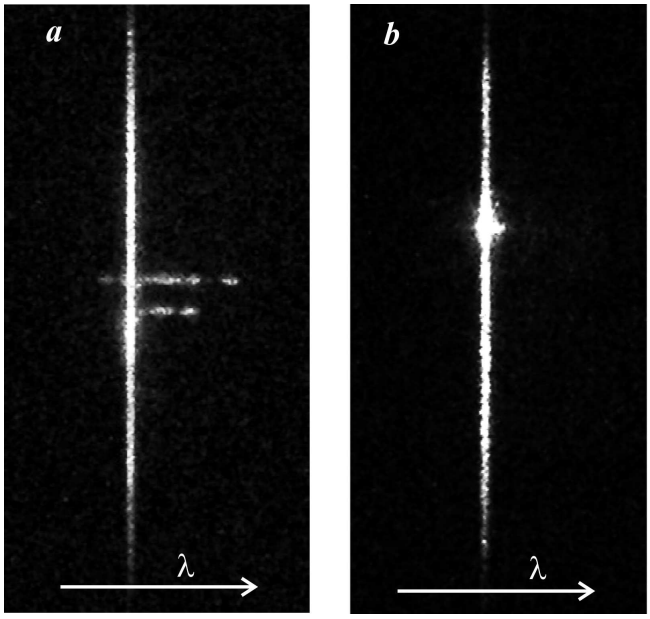

Fig. 4. Photos of the spectra of the laser emission at the outlet of a 0.25-m cell with toluene for $E_i/E_{i,\max} = 0.75$ (a) and 0.52 (b). The arrows show the direction of increasing λ

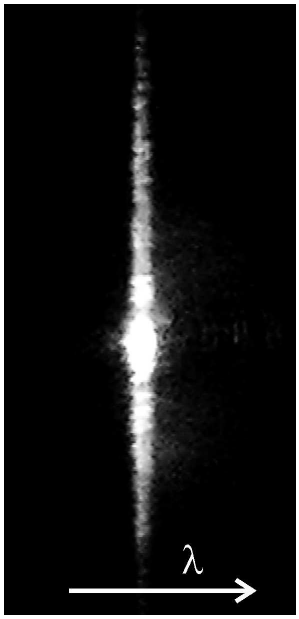

Fig. 5. Photo of the laser emission spectrum from the depth of a cell filled with toluene

The spectra of the laser emission are shown in Fig. 4 for $L = 25$ cm and various energies of laser pulses $E_i = 0.75E_{i,\max}$ (a) and $0.52E_{i,\max}$ (b). Here, the vertical line is the image of the spectrograph slit at the wavelength λ_0. The horizontal strips correspond to the spectral broadening of the emission from the local sites of the beam, i.e. the focal regions that arise owing to the small-scale SF. The maximal spectral broadening $\Delta\nu_{\max}$ equals 53 cm^{-1} towards the Stokes and 13 cm^{-1} towards the anti-Stokes side (the upper strip) in Fig. 4,a; and 6 cm^{-1} towards only the Stokes side in Fig. 4,b. A prevailing and even exclusive broadening towards the Stokes side was a typical feature of every spectrum.

The different kinds of the spectra in Figs. 4,a and b reflects a general tendency: the reduction of E_i is accompanied by a reduction of the spectral broadenings and an increase of the brightness of the focal region images at the laser emission frequency. At the SF threshold, only the bright images of the focal region were observed at the wavelength λ_0, while the spectral broadenings were absent. This evidences for a close connection between the broadening amplitude and the velocity, with which the focal region crosses the cell boundary. It is so, because the focal point emerges and disappears at the SF threshold depending on L at the cell boundary and has zero velocity.

Changing the cell length from 25 to 12.5 cm led to a reduction of the Stokes spectral broadenings from 74 down to 18 cm^{-1} (the average values), provided that $E_i = E_{i,\max}$. We notice that the shorter the cell, the smaller is v_f at the cell outlet and the larger is the instant power of the laser at that moment. Therefore, it is obvious that the velocity, with which the focal region crosses the air—Kerr liquid interface, is more important than the instant power of the laser at this moment.

In the case where the deep cross-sections of the cell, which were located at a distance up to 12 cm from the inlet window, were projected onto the spectrograph slit, the spectra possessed diffusive character (Fig. 5, a distance of 11.25 cm) and did not contain the frequency broadenings typical of the cell outlet. This also confirms a connection between such broadenings and the transition effect occurring at the phase self-modulation of emitted pulses.

Fig. 6 summarizes the results of studies of the dependence of the maximal frequency broadening $\Delta\nu_{\max}$ towards the Stokes side on $\tilde{P}$ at $L = 25$ and 12.5 cm. The points corresponding to the average values of $\Delta\nu_{\max}$ are plotted, and the relevant standard errors are indicated. Under real experimental conditions and provided maximal E_i and L, every spectrum demonstrated up to 10 focal regions and the corresponding local spectra of various broadenings owing to a reduction of the beam fragment power while moving away from the beam center. The procedure of the preliminary selection of the data consisted in determining, for every spectrum, the position of the outermost maximum at the Stokes

threshold of the spectrum for the focal region which generated the radiation with the greatest frequency broadening. Upon the further averaging, the zero results, if any (for low values of E_i), were rejected. This was done, because there might be a finite probability for none of the focal regions that had crossed the outlet window of the cell to be projected onto the spectrograph slit.

The satisfactory quantitative agreement between the experimental data and the theoretical results (Fig. 6) were achieved at the following parameters: 1) the duration of the Gaussian-like pulse of emission was $2\tau = 2$ ns at the $1/e$-level, 2) the initial radius of the beam fragment which self-focused was $a_0 = 113$ μm, and 3) the excess of the critical power at the top of the pulse was $\tilde{P} = 2.35$ (this value was associated with $E_i = E_{i,\max}$). Such parameters are real if one takes into account that there is a secondary longitudinal mode in the laser radiation, and that the beam is non-uniform over its cross-section. The calculations were carried out by using the approximated formula (17) (the dotted curve) and finding the extreme value of the instant frequency incursion with the use of Eqs. (7) and (8) (the solid curves). The disagreement of the theoretical and experimental results for the smallest $\tilde{P}$ value ($L = 25$ cm) can be explained by the fact that our calculations were based on the formulae which give an exact result provided $\tilde{P} \geq 1.5$ [8]. Moreover, the calculations were carried out for the radiation along the axis, while the radiation was registered within the angular range of $\pm(40 - 70)'$. We note that the same level of agreement between the experimental data and the theoretical results can be achieved, as well, if three other indicated parameters are varied, retaining their correlation, up to 20%; for example, $2\tau = 1.7$ ns, $a_0 = 130$ μm, and $\tilde{P} = 2.65$.

Among other experimental results, important are those related to the observation of the anti-Stokes component in the SRS spectra. Contrary to the laser emission radiation, the spectra of the anti-Stokes components from the focal regions included significant frequency broadenings (some hundreds of cm^{-1} units towards the Stokes side), when the deep cross-sections of the cell were projected onto the spectrograph slit.

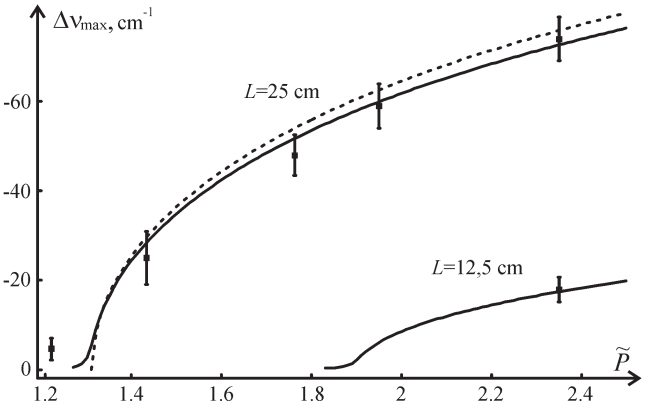

Fig. 6. Comparison of experimental and theoretical results for the Stokes value of $\Delta\nu_{\max}$. The dotted curve corresponds to calculations by Eq. (17), and the solid curves to calculations by Eqs. (7) and (8)

4. Conclusions

The experimental data obtained prove that, owing to the quasi-stationary self-focusing at the phase self-modulation of laser pulses within a nanosecond range, the transition effect is responsible for the generation of new spectral components shifted by up to about 100 cm^{-1}, mainly towards the Stokes side with respect to the frequency of the stimulating radiation.

The main evidences for the direct connection between the transition effect and the registered spectral broadenings are the following: (i) the power reduction was accompanied by a reduction of the broadenings and by an essential increase of the brightness of the focal region images at the laser emission frequency; (ii) the shortening of the cell length resulted in a reduction of the maximal spectral broadenings; (iii) if the deep cross-sections of the cell were projected onto the spectrograph slit, the spectra did not include the frequency broadenings of the laser component, which are typical of those at the cell outlet; (iv) the experimental data and the theoretical results are in a satisfactory quantitative agreement; and (v) there is no close correlation between the spectral broadenings of the laser and anti-Stokes components.

The asymmetry of the laser component broadenings owing to the transition effect is connected, in our opinion, to the inertia of the Kerr effect (because the focal region crosses the boundary for about 10 ps) and the exhaustion of the laser radiation in the course of the SRS process at the moment of the pulse dropping, when the focal region crosses the cell boundary backwards.

1. *Shen Y.R.* The Principles of Nonlinear Optics. — New York: Wiley, 1984.

2. *Akhmanov S.A., Vysloukh V.A., Chirkin A.S.* Optics of Femtosecond Laser Pulses. — Moscow: Nauka, 1988 (in Russian).

3. *Ivanisik A.I., Malyi V.I., Ponezha G.V.* // Opt. Spektr. — 1996. — **80**, N 2. — P. 212—217.

4. *Kandidov V.P., Golubtsov I.S., Kosareva O.G.* // Quant. Electr. — 2004. — **34**, N 4. — P. 348—354.

5. *Gustafson T.K., Taran J.P., Haus H.A. et al.* // Phys. Rev. — 1969. — **177**, N 1. — P. 306—313.

6. *Shimoda K.* // Jpn. J. Appl. Phys. — 1966. — **5**, N 7. — P. 615 — 623.

7. *Ivanisik A.I., Malyi V.I., Ponezha G.V.* // Opt. Spektr. — 1998. — **85**, N 3. — P. 512—516.

8. *Dawes E.L., Marburger J.H.* // Phys. Rev. — 1969. — **179**, N 3. — P. 862—868.

9. *Ivanisik A.I., Malyi V.I., Ponezha G.V.* // Opt. Spektr. — 1998. — **85**, N 1. — P. 88—94.

Received 15.03.05.
Translated from Ukrainian by O.I. Voitenko

ПЕРЕХІДНИЙ ЕФЕКТ НА МЕЖІ ПОДІЛУ СЕРЕДОВИЩЕ—ВАКУУМ В УМОВАХ ФАЗОВОЇ САМОМОДУЛЯЦІЇ СВІТЛОВОГО ІМПУЛЬСУ

С.О. Дудка, А.І. Іванісік, А.В. Конопатський, П.А. Коротков

Р е з ю м е

Розглянуто фазову самомодуляцію наносекундних імпульсів лазерного випромінювання в умовах квазістаціонарного самофокусування (СФ) у керрівській рідині. Проведено розрахунки для додаткової затримки фази, миттєвої частоти та спектра імпульсу. Розрахунки та отримані експериментальні дані свідчать про наявність перехідного ефекту, відповідального за нові спектральні компоненти на межі середовища. Ці спектральні компоненти зміщені приблизно на 100 $см^{-1}$ у стоксовий бік відносно частоти збуджуючого випромінювання. Незважаючи на можливе суттєве частотне розширення імпульсів, найбільша спектральна густина енергії припадає на незміщену частоту.